INSTRUMENTATION AND MEASUREMENT

Application of silicon carbide temperature monitors in 49-2 swimming-pool test reactor

Guang-Sheng Ning(宁广胜)[1], Li-Min Zhang(张利民)[2,†], Wei-Hua Zhong(钟巍华)[1,‡], Sheng-Hong Wang(王绳鸿)[2], Xin-Yu Liu(刘心语)[3], Ding-Ping Wang(汪定平)[2], An-Ping He(何安平)[3], Jian Liu(刘健)[1], and Chang-Yi Zhang(张长义)[1]

[1] *Reactor Engineering Technology Research Institute, China Institute of Atomic Energy, Beijing* 102413, *China*
[2] *School of Nuclear Science and Technology, Lanzhou University, Lanzhou* 730000, *China*
[3] *School of Information Science and Engineering, Lanzhou University, Lanzhou* 730000, *China*

(Received 5 December 2022; revised manuscript received 13 January 2023; accepted manuscript online 18 January 2023)

High purity SiC crystal was used as a passive monitor to measure neutron irradiation temperature in the 49-2 research reactor. The SiC monitors were irradiated with fast neutrons at elevated temperatures to 3.2×10^{20} n/cm^2. The isochronal and isothermal annealing behaviors of the irradiated SiC were investigated by x-ray diffraction and four-point probe techniques. Invisible point defects and defect clusters are found to be the dominating defect types in the neutron-irradiated SiC. The amount of defect recovery in SiC reaches a maximum value after isothermal annealing for 30 min. Based on the annealing temperature dependences of both lattice swelling and material resistivity, the irradiation temperature of the SiC monitors is determined to be $\sim$ 410 °C, which is much higher than the thermocouple temperature of 275 °C recorded during neutron irradiation. The possible reasons for the difference are carefully discussed.

Keywords: silicon carbide, irradiation temperature monitor, research reactor

PACS: 61.80.Hg, 28.52.Lf, 28.50.Dr **DOI:** 10.1088/1674-1056/acb41c

1. Introduction

Silicon carbide (SiC) crystal can be used as a passive irradiation temperature monitor in test reactors. SiC monitors were first conceived in 1960s[1,2] and they regained research interesting in the past two decades,[3–9] especially after the disaster of Fukushima, because precise knowledge of irradiation temperature is critically important to the evaluation of radiation damage in nuclear materials. The advantages of SiC monitors are that they have a smaller size, a lower gamma heating rate and a lower residual radioactivity as compared to other passive monitors, such as melt wires and paint spots.[10] More importantly, they provide a wide range for temperature measurement, which showed measurement accuracies of 10–100 °C over a temperature range from 200 °C to 800 °C.[8–12] In practice, since voids are not formed in SiC when irradiated with neutrons at temperatures up to 1250 °C,[13] the maximum measurement temperature of SiC can be extended to a higher value, which is highly desired for the application in advanced reactors.

The underlying physical mechanism of SiC monitors is that neutron irradiation damage in SiC starts to be recovered when post-irradiation annealing temperature exceeds irradiation temperature. The damage recovery can be characterized by the changes in sample length, density, thermal diffusivity, lattice spacing and electrical resistivity. The latter two are most commonly used because of their ease of application, which involve conventional x-ray diffraction (XRD) and four-point probe resistance measurements. The electrical resistivity method is also superior in measuring temperature with very low neutron fluences. For instance, the irradiation temperature was successfully estimated by electrical analysis of SiC with a neutron fluence of 1.5×10^{17} n/cm^2 ($E > 0.18$ MeV),[11] whereas neutron fluences of $> 1.5 \times 10^{19}$ n/cm^2 are usually required for the other methods based on structural changes in SiC, such as XRD.[3,4] Despite many advantages, the acquisition of irradiation temperature from a SiC monitor needs repetitive sample testing after sequential annealing processes. It is time consuming and will introduce additional error sources due to the repeated transfer of the monitor between the annealing and testing systems.[7] In order to improve the measurement methods, efforts have been made to develop automatic techniques by continuously examining the length and electrical resistivity of the SiC monitor in real-time heating/cooling cycles.[5–7] Alternatively, it was proposed that the irradiation temperature of the SiC monitors can be inferred by analyzing the saturated swelling rate of SiC without annealing treatment, as the volume swelling is inversely proportional to the irradiation temperature.[4] However, plenty of experimental data are needed to calibrate the swelling vs. temperature curves for the different types of SiC. This paper reports on the development

[†]Corresponding author. E-mail: zhanglm@lzu.edu.cn
[‡]Corresponding author. E-mail: zhongwh@ciae.ac.cn

© 2023 Chinese Physical Society and IOP Publishing Ltd

and utilization of SiC monitors in the 49-2 swimming-pool reactor at the China Institute of Atomic Energy (CIAE). Both the lattice spacing and electrical resistivity methods were used to determine the irradiation temperature of the SiC monitors. In addition, the isochronal and isothermal annealing analyses of the SiC monitors were conducted to investigate the optimal post-irradiation annealing parameters, which is critical to the use of SiC monitors.

2. Experimental details

Both α and β phase SiC can be used for temperature monitors.[9,10] In this work, the SiC monitors were fabricated using high-purity ($>$ 99.9995%), full-density and high-resistance polycrystalline 6H-SiC. The grain sizes in SiC range from 0.5 μm to 4 μm. The SiC material was shown to be n-type by hot-probe measurements using the ST-13 multifunctional sort of semiconductor tester and the material electrical resistivity at room temperature is $>$ 1200 Ω·cm. The SiC monitors were machined in bar-form to facilitate the four-point probe measurements, as illustrated in Fig. 1. Neutron irradiation was performed in hole D10 of the 49-2 swimming-pool test reactor at the CIAE. A stainless-steel capsule was designed to contain the SiC samples, together with a temperature compensation system to maintain the irradiation temperature (see Fig. 1). During irradiation, the target temperature was monitored by an *in-situ* thermocouple that is fixed in the center of the sample holders. The samples were irradiated with fast neutrons ($>$ 0.1 MeV) to 3.2×10^{20} n/cm^2 at a flux of 1.35×10^{13} (n/cm^2)/s. The irradiation leads to a dose of 0.32 dpa in SiC, as calculated by the SPECTER code[14] with the assumptions of the threshold displacement energies of 20 eV and 35 eV on the C and Si sublattices,[15] respectively. According to the temperature record from the *in-situ* thermocouple, the SiC sample was first irradiated to a dose of 0.12 dpa at 290 °C and then to another dose of 0.2 dpa at a decreased temperature of 275 °C.

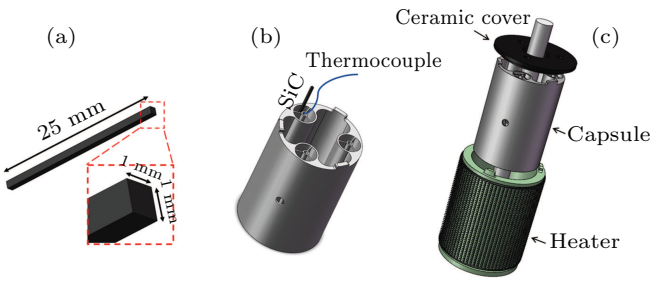


Fig. 1. Sketches of (a) SiC monitor, (b) irradiation capsule and (c) temperature compensation system.

After irradiation, tubular vacuum annealing furnaces were used for sample annealing. Prior to annealing, calibration of sample temperature was performed by a thermocouple fixed on crucible in the furnaces. The samples were annealed at various temperatures ranging from 400 °C to 1000 °C for different duration time from 3 min to 120 min. In order to control the isothermal annealing time, the furnace was heated to the designated temperatures and then the samples were inserted into the furnace; after annealing to the designated time, the samples were removed from the furnace and kept in the sealed tube under a vacuum of 2×10^{-5} Pa. The structure and electrical property of the SiC monitors have been characterized by transmission electron microscopy (TEM), XRD and four-point probe techniques. Cross-sectional TEM specimens were prepared using a focused ion beam system. FEI TF20 TEM was employed for imaging at an accelerating voltage of 200 kV. Using a Rigaku SmartLab diffractometer with a Cu anode operating at 40 kV and 40 mA, grazing-angle incidence x-ray diffraction (GIXRD) at a fixed angle of $\omega = 3°$ was conducted to analyze the samples. Asymmetric scans were made in the range of 2θ from 50° to 70° with a step of 0.01° per 0.12 s. The penetration depth of the x-rays was obtained following the method proposed in Ref. [16], assuming that the absorption coefficient of the Cu $K\alpha$ lines in SiC is 211 cm^{-1}.[17] The penetration depth for $\omega = 3°$, averaged over the range of the measured diffraction angles, is estimated to be 2.33 μm. The GIXRD measurements were repeated after each sequence of sample annealing. In order to minimize the influence of grain orientation in the polycrystalline SiC samples, the samples were carefully loaded in the same configuration for each measurement. Using four-point probe method, the sample electrical resistivity was measured at 30 °C in a constant temperature chamber, as illustrated in Fig. 2.

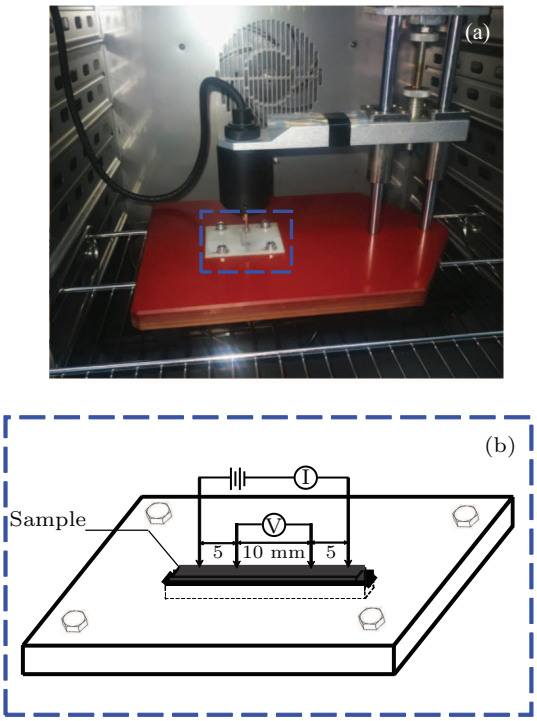


Fig. 2. (a) Experimental setup and (b) a sketch map for the electrical resistivity measurements of the SiC monitors.

Four in-line and spring-pressed probes are brought in contact with the sample surface that is fixed into a slot of the sample holder. Two outer probes are used to source current using a Keithley 6221 DC current source, whereas two inner probes are used to measure voltage using a 2182A nanovoltmeter. Ohmic contact of the probes on SiC was established by pre-testing the current vs. voltage curve. Prior to the electrical measurements, the SiC monitors were bathed in 10% HF acid for 30 min to remove silica (if any) on the sample surface.

3. Results and discussion

Figure 3 shows the typical cross-sectional high-resolution TEM (HRTEM) images taken in the bulk of the SiC samples before and after neutron irradiation to 0.32 dpa at temperatures between 290 °C and 275 °C. The unirradiated SiC exhibits a clear lattice pattern, in which the mottled contrast is due to lattice stress probably induced by a low density of pre-existing defects. In addition, the lattice damage could be produced by ion milling of the TEM foils. After irradiation, no significant changes are revealed in the TEM image. Invisible point defects and small defect clusters should be the dominant defect types in SiC at the applied irradiation temperature and dose.[18] Most of the defects are unresolvable by the conventional TEM. However, XRD and electrical resistivity measurements are very sensitive to those defects, which provides the opportunities for temperature measurements, as shown below.

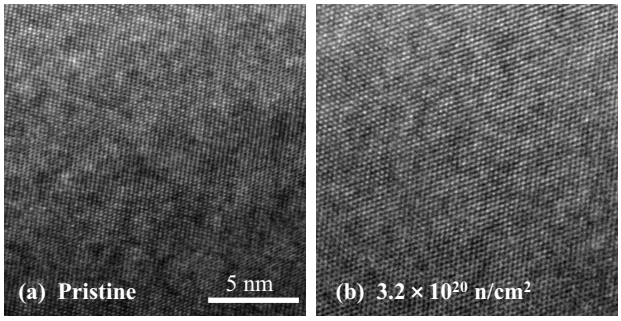


Fig. 3. Cross-sectional HRTEM images of (a) the unirradiated and (b) neutron-irradiated SiC. The two images have the same scalar bar.

Figure 4(a) shows the GIXRD patterns of the neutron-irradiated SiC monitors before and after isochronal annealing at typical temperatures for 30 min. The data from the unirradiated SiC is also included for comparison. The XRD patterns exhibit a pair of 6H-SiC (110) peaks that correspond to the Cu $K\alpha_1$ and $K\alpha_2$ irradiations. After irradiation, the diffraction peaks are shifted to smaller angles significantly, indicating an irradiation-induced lattice expansion in SiC. The peak position of the irradiated SiC keeps unchanged after post-irradiation annealing until the annealing temperature exceeds the irradiation temperature, above which the diffraction peaks gradually shift to the large angle direction with increasing annealing temperature.

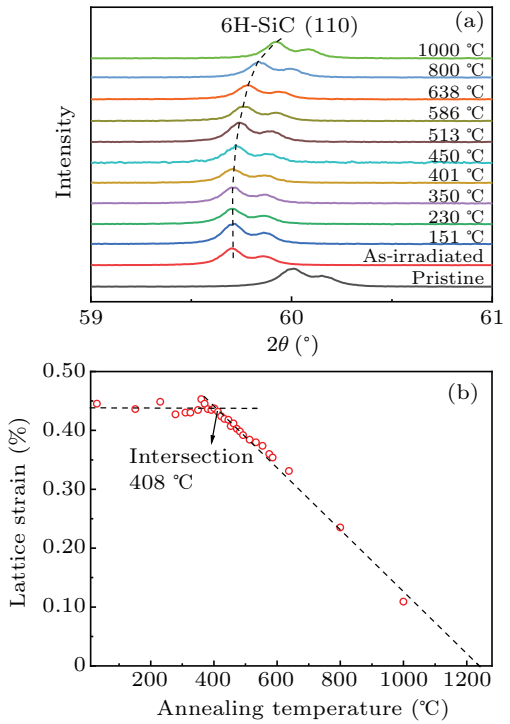


Fig. 4. (a) GIXRD patterns for the SiC before and after the neutron irradiation and subsequent annealing at various temperatures. A dash line is drawn to guide the eye. (b) Plot of the lattice strain versus isochronal annealing temperature for the neutron-irradiated SiC monitor. The dash lines are linear fits to data points.

Based on the GIXRD data in Fig. 4(a), the relative lattice strain in SiC is estimated by $[(d-d_0)/d_0 \times 100\%]$, where d_0 is the (110) d-spacing of the pristine SiC, and d is the value after neutron irradiation and subsequent annealing. Figure 4(b) shows the calculated lattice strain as a function of annealing temperature. It is seen that the lattice strain begins to decrease when the annealing temperature surpasses the irradiation temperature. Note that the width of the annealing steps is reduced to 5 °C around the point of deflection to track the irradiation temperature more precisely. Beyond the deflection point, the lattice strains decrease linearly with increasing annealing temperature. Complete annealing of the SiC is expected to occur at 1239 °C according to the linear relationship. The linear dependence of lattice strain on annealing temperature has been explained by a demarcation energy model.[4] In that model, it is assumed that there is a demarcation energy that is proportional to the sample temperature; the radiation defects in SiC with the activation energy lower than the demarcation energy are annealed out, whereas the defects with the higher activation energy remain to cause the residual lattice swelling. In order to determine the irradiation temperature, the data points in Fig. 4(b) are fitted by two straight lines using the least-squares method. The intersection temperature of 408 °C is specified as the irradiation temperature, which is significantly higher than the values of 275–290 °C recorded by thermocouple during irradiation.

Figure 5 shows the changes in lattice strain for the neutron-irradiated SiC monitors annealed at 450 °C, 586 °C

and 638 °C for different duration time. It is seen that for all the three temperatures, the lattice strain in SiC decreases rapidly at initial time within 3 min. After that, the lattice strain continues to decrease at a very low rate until the steady values are achieved after a period of 30 min. Further increase in annealing time leads to little changes in lattice strain. It suggests that the defective structure in neutron-irradiated SiC has been stabilized after annealing for 30 min. This is consistent with the results previously observed in cubic phase 3C-SiC,[2] which shows the maximum recoveries in length and thermal diffusivity of neutron-irradiated SiC after annealing for 30 min. Actually, the local configurations in 6H- and 3C-SiC are the identical CSi_4 and SiC_4 tetrahedrons, and therefore they have similar disorder accumulation and recovery processes, as evidenced by the heavy ion irradiation and subsequent thermal annealing.[19,20]

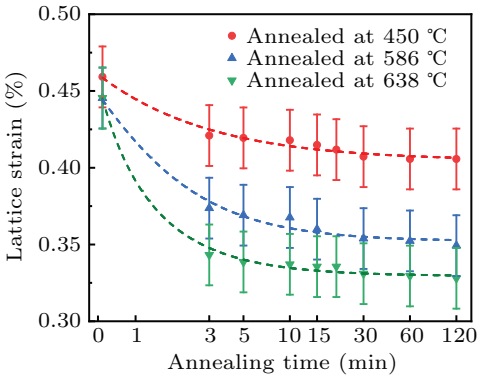


Fig. 5. Plots of the lattice strain versus isothermal annealing time for the neutron-irradiated SiC monitors. Dash lines are drawn to guide the eyes. The uncertainties of the data points are due to the precision of the XRD measurement that has an angular resolution of 2θ of 0.01°.

Figure 6(a) shows the *I*–*V* curves of the pristine and neutron-irradiated SiC after annealing at various temperatures. No changes in resistance are detected for the pristine SiC after annealing and also for the neutron-irradiated SiC after annealing at 300 °C and 350 °C. So the corresponding *I*–*V* curves for those annealed samples are omitted in Fig. 6(a) for clarity. The lower currents are applied on the neutron-irradiated SiC annealed at 580 °C and 630 °C because of the large resistance of the samples. The electrical resistivity of the SiC monitor is calculated from the *I*–*V* curves. Figure 6(b) shows the resistivity of the pristine and irradiated SiC as a function of annealing temperature. The resistivity of the unirradiated SiC keeps unchanged after annealing in the applied temperature range. It indicates that the resistance measurement does not suffer from the surface oxidation of the SiC samples that have been pretreated by bathing in HF. The neutron irradiation leads to a significant increase in resistivity of SiC, which is attributed to the radiation damage produced by fast neutrons.[21] The sample resistivity begins to increase when it is heated above the irradiation temperature, which is owing to the elimination of the mobile interstitials (especially C interstitials) that act as donors in SiC.[3,22] Using the lines-of-intersection approach, the irradiation temperature based on the resistivity data is determined to be 436 °C, which is higher than the value of 408 °C obtained by XRD in Fig. 4(b). In fact, different from the linear dependence of lattice swelling on annealing temperature, the sample resistivity increases with annealing temperature in a supralinear fashion. So the onset temperature, where the sample resistivity starts to increases with annealing, was recommended to be taken as the irradiation temperature.[9] In Fig. 6(b), the onset temperature is distinguished as ∼ 400 °C, which is close to the value obtained from the XRD analysis.

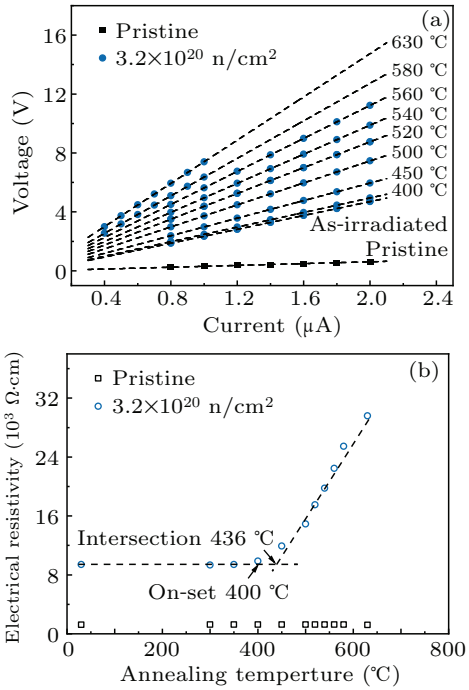


Fig. 6. (a) The *I*–*V* curves for the pristine and neutron-irradiated SiC after annealing at various temperatures. (b) Annealing temperature dependence of the electrical resistivity for the pristine and neutron-irradiated SiC. The dash lines are linear fits to data points.

In the present study, the SiC temperature during neutron irradiation is not constant. The initial irradiation temperature recorded by *in-situ* thermocouple is 290 °C with a dose of 0.12 dpa, and then it decreases to 275 °C with another dose of 0.2 dpa. As a result, the radiation defects created at 290 °C are frozen in SiC, while new defects will be produced at 275 °C and tend to saturate at the dose of 0.2 dpa.[2] In principle, the SiC monitors only indicate the irradiation temperature at the end of irradiation.[8] So the SiC monitors used in this work give an overestimate of ∼ 135 °C than the thermocouple temperature. It was found that the accuracy of SiC monitors depends on the neutron irradiation temperature and post-irradiation annealing conditions.[8–10] Basically, the higher the temperature of neutron irradiation, the lower the accuracy of SiC monitors. This is because neutron irradiation at the higher temperature leads to less absolute changes in structure and properties of SiC. For the low-temperature neutron

irradiation applied in this work, the irradiation-induced lattice strain of SiC is as large as ~ 0.45 and the sample resistivity is increased by one order of magnitude, which is sufficient for the precise determination of the irradiation temperature. Regarding the post-irradiation annealing, it is seen from Fig. 5 that the amounts of defect recovery in SiC have reached maximum values after annealing for 30 min. These results suggest that the overestimate is not due to the nature of neutron irradiation and sample annealing. Since the structural and electrical analyses of the SiC monitors yield similar irradiation temperature values, the overestimate is not related to the measurement methods themselves, either. It was proposed that the data analysis with the simple application of intersection of isochronal annealing lines could lead to a considerable overestimate of irradiation temperature.[9] Efforts have been devoted to writing data analysis software that standardizes the analysis.[6] Nevertheless, it is important to note that in the present work, the *in-situ* thermocouple during neutron irradiation is not in direct contact with the SiC monitors, but fixed on the sample holder instead (see Fig. 1). A difference probably exists in temperature between the SiC monitor and thermocouple. Further investigations with thermocouple fixed on SiC are needed to clarify the error origin.

4. Conclusions

This study reports on the use of passive SiC temperature monitor in 49-2 research reactor at the CIAE. Both the lattice spacing and electrical resistivity methods have been utilized to determine the irradiation temperature of the SiC monitors. Isochronal and isothermal annealing experiments were also performed on the irradiated SiC monitors to investigate the optimal annealing conditions. The neutron irradiation at nominal 275 °C to 0.2 dpa leads to significant lattice swelling in SiC, where point defects and smaller defect clusters are the dominant defect types. The recovery of radiation defects in SiC saturates after isothermal annealing for 30 min. The structural and electrical analyses of the SiC monitors give similar irradiation temperature values of ~ 410 °C, which, however, is significantly higher than that of 275 °C recorded by *in-situ* thermocouple. The difference is partly due to the configuration of the designed irradiation capsule, where the thermocouple is fixed on the sample holder but not in direct contact with the SiC monitor. In addition, the conventional data analysis method that involves a simple lines-of-intersection approach needs to be improved.

Acknowledgements

The authors thank the staff of the swimming-pool test reactor at the CIAE for the support of the neutron irradiation. We are grateful to Prof. Chun-Lei Wang at the Tsinghua University for his great help to this work.

References

[1] Pravdyuk N F, Nikolaenko V A, Kapuchin V I and Kapuchin V N 1962 *Properties of reactor materials and the effects of radiation damage*, (London: Butterworths Press) p. 57
[2] Thorne R P, Howard V C and Hope B 1967 *Proc. Br. Ceram. Soc.* **7** 449
[3] Ning G, Zhang L, Zhong W, Wang S, Liu J and Zhang C 2022 *Nucl. Instr. Meth. Phys. Res. B* **512** 91
[4] Gusarov A, Davis K L, Pitte J V, Heidrich B J, Uytdenhouwen I and Dyck S V 2020 *J. Nucl. Mater.* **542** 152535
[5] Wang H, Koyanagi T, Geringer J W, Campbell A A and Katoh Y 2020 *J. Nucl. Mater.* **540** 152370
[6] Campbell A A, Porter W D, Katoh Y and Snead L L 2016 *Nucl. Instr. Meth. Phys. Res. B* **370** 49
[7] Daw J, Unruh T and Rashdan A A 2016 *Silicon carbide temperature monitor process improvements*, INL/EXT-15-36738
[8] Rempe J L, Condie K G, Knudson D L and Snead L L 2010 *IEEE T. Nucl. Sci.* **57** 1589
[9] Snead L L, Williams A M and Qualls A L 2003 *Revisiting the use of SiC as a post irradiation temperature monitor, Effects of Radiation on Materials*, ASTM STP 1447, Grossbeck M L, Ed, ASTM International, West Conshohocken, PA
[10] Price R J 1972 *Nucl. Technol.* **16** 536
[11] Suzuki H, Iseki T and ITO M 1973 *J. Nucl. Mater.* **48** 247
[12] Palentine J E 1976 *J. Nucl. Mater.* **61** 243
[13] Snead L L, Nozawa T, Katoh Y, Byun T S, Kondo S and Petti D A 2007 *J. Nucl. Mater.* **371** 329
[14] Greenwood L R 1994 *J. Nucl. Mater.* **216** 29
[15] Devanathan R, Weber W J and Gao F 2001 *J. Appl. Phys.* **90** 2303
[16] Rafaja. D, Valvoda V, Perry A J and Treglio J R 1997 *Surf. Coat. Tech.* **92** 135
[17] Intarasiri S, Yu L D, Singkarat S, Hallén A, Lu J, Ottosson M, Jensen J and Possnert G 2007 *J. Appl. Phys.* **101** 084311
[18] Sprouster D J, Koyanagi T, Dooryhee E, Ghose S K, Katoh Y and Ecker L E 2017 *Scripta Mater.* **137** 132
[19] Debelle A, Thomé L, Dompiont D, Boulle A, Garrido F, Jagielski J and Chaussende D 2010 *J. Phys. D: Appl. Phys.* **43** 455408
[20] Jiang W, Weber W J, Lian J and Kalkhoran N M 2009 *J. Appl. Phys.* **105** 013529
[21] Hazdra P, Záhlava V and Vobecky J 2014 *Nucl. Instr. Meth. Phys. Res. B* **327** 124
[22] Chen X D, Fung S, Ling C C, Beling C D and Gong M 2003 *J. Appl. Phys.* **94** 3004